Research Square

Preprints are preliminary reports that have not undergone peer review.
They should not be considered conclusive, used to inform clinical practice,
or referenced by the media as validated information.

The metabolic milieu of tuberculosis-type 2 diabetes mellitus comorbidity using ^{1}H-NMR metabolomics

Stephan Terblanche
North-West University
Shayne Mason
North-West University
Léanie Kleynhans
Stellenbosch University
Katharina Ronacher
Stellenbosch University
Du Toit Loots
dutoit.loots@nwu.ac.za

North-West University

Article

Keywords: Tuberculosis, type-2 diabetes mellitus, metabolomics, comorbidity, 1H-NMR

Posted Date: April 1st, 2026

DOI: https://doi.org/10.21203/rs.3.rs-9167983/v1

License: This work is licensed under a Creative Commons Attribution 4.0 International License. Read Full License

Additional Declarations: No competing interests reported.

Abstract

Background

The prevalence of tuberculosis (TB) and type 2 diabetes mellitus (T2DM) comorbidity (TB-T2DM) is on the rise globally and negatively impacts disease progression and treatment outcomes for both diseases. T2DM additionally increases the risk of developing active TB and can double the risk of death from TB, and vice versa. A major contributing factor to the growing global prevalence of TB-T2DM is the dearth of knowledge regarding the metabolic interaction of these two diseases and the combined impact on host metabolism.

Methods

This study aimed to broadly characterise the urinary metabolic profiles of TB-T2DM comorbid patients in a South African cohort using untargeted proton nuclear magnetic resonance spectroscopy (^{1}H-NMR) metabolomics, by comparing 30 healthy controls and 14 patients with both TB and T2DM.

Results

Principal component analysis showed the control and comorbid groups as distinct clusters, and 23 urinary metabolites were identified as significantly increased in TB-T2DM versus healthy controls using univariate statistical analyses. The metabolite markers identified indicate inhibited glycolysis (glucose, mannose, sucrose) and tricarboxylic acid (TCA) cycle functionality (citrate, α-ketoglutarate, succinate and fumarate), accompanied by an elevated gluconeogenesis (glucose, pyruvate, lactate, alanine), muscle wasting/amino acid catabolism (leucine, valine, isoleucine, and tyrosine), kidney damage (creatinine, methylguanidine), alterations in gut microbial/one-carbon metabolism (choline, trimethylamine, trimethylamine-N-oxide, dimethylamine and methylamine), ketogenesis (β-hydroxybutyrate), and potentially altered carnitine reabsorption (carnitine). This study further suggests the previously proposed imbalance in the NAD^{+}/NADH ratio, which is an important outcome that warrants further investigation.

Conclusion

Overall, this study indicates that the TB-T2DM metabolic changes result from a compounded metabolic effect of both diseases, although some metabolite alterations are more closely associated with those previously seen in T2DM. This study subsequently expands the current understanding of the TB-T2DM comorbid metabolic milieu and identifies new avenues for future research, for a better understanding of the individual effects of each disease and their combined impact in patients with TB-T2DM comorbidity.

Background

Tuberculosis (TB) and type 2 diabetes mellitus (T2DM) place a significant burden on healthcare resources globally. In 2023, an estimated 10.3 million new TB cases were reported worldwide (1). As of 2024, the global prevalence of diabetes was estimated at 589 million people, and this number is projected to increase to 853 million by 2050 (2). The convergence of these two diseases, particularly in low-and-middle income countries that have high TB and diabetes burdens, increases the prevalence of the tuberculosis-type 2 diabetes mellitus comorbidity (TB-T2DM). In 2021, the global prevalence of TB in previously diagnosed T2DM patients was reported to be 13.73% (3), with an average 4.1% occurrence of diabetes in patients previously diagnosed with TB (4), and highly variable regional statistics highlighting the roles of lifestyle, genetics, age, sex, etc. (5).

TB is primarily a pulmonary infectious disease spread by inhaled aerosol droplets containing the bacterium *Mycobacterium tuberculosis* (*Mtb*) (6). In most individuals, the infection is contained by the host's immune system, a condition termed latent or subclinical TB (7), but factors such as alcohol abuse, smoking, diabetes mellitus and malnutrition significantly contribute to the development of active TB (8). T2DM is a risk factor for TB. Patients with T2DM are more likely to become infected with *Mtb* (9), develop active TB when they become infected, and to fail TB treatment or die (10–12). Patients with T2DM also have an increased risk of developing drug-resistant TB (13). Diabetes mellitus, of which 90–95% constitutes T2DM (2), is marked by hyperglycaemia with a progressive loss of insulin sensitivity, chronic inflammation, pancreatic β-cell damage, and eventually a diminished insulin-producing capacity (14, 15). Anti-TB and anti-T2DM drugs have furthermore been shown to have detrimental interactions, lowering treatment success (16, 17). To better understand this complex disease interaction, urinary, plasma, serum, or sputum metabolomics can be used to infer the pathophysiological mechanisms underlying the interaction between these two diseases (18).

The human metabolic profiles of TB (19–23) and T2DM (24–26) have been extensively characterised, indicating that both diseases independently cause significant changes to glycolysis, gluconeogenic flux, proteolysis, amino acid catabolism, the TCA cycle, gut microbial metabolic pathways, and the urea cycle. However, to date, most metabolomics studies in the context of T2DM or TB have used serum or plasma (21, 25, 27–32), with a few using urine (22, 26, 33–36). Considering the TB-T2DM comorbidity, very few metabolomics studies have been conducted to date (37, 48, 49). These studies used patient plasma and identified metabolic profiles resembling those previously reported in TB and/or T2DM. TB-T2DM metabolic profiles were indicative of significant muscle and amino acid wasting (increased branched-chain amino acids (BCAAs), tyrosine and phenylalanine, and decreased threonine, alanine, histidine and glutamine), dysglycaemia (increased glucose with decreased serine, glycine, homoserine and alanine), urea cycle alterations (decreased ornithine and citrulline), and gut microbial dysbiosis (reduced choline) (37, 38). A GCxGC – TOFMS metabolomics study by Reinecke *et al.* (39), using the same patient cohort as our study, found alterations in the tryptophan pathway, NAD^{+} synthesis, nucleotide salvage pathways, glycine conjugation, BCAA and fatty acid catabolism, tyrosine utilisation, and the gut microbiome in the TB-T2DM patients relative to healthy controls (HC). However, given gas chromatography's bias toward non-polar metabolites (40) and its limited applicability for confidently detecting carbohydrates, an unbiased analytical platform such as ^{1}H-NMR (41), as applied in this investigation, would provide additional information regarding the metabolic perturbations in TB-T2DM patients.

Blood provides a broad view of the metabolic state at a particular point in time (42), while urine is less susceptible to rapid metabolic changes (43), contains markers indicative of various physiological abnormalities, such as an altered kidney function (44), and can, in some cases, be used for earlier disease detection than blood assays (45). Urine has also been shown to be suitable for diabetes risk assessment, diagnostic biomarker detection, and disease progression studies (46, 47). Non-invasive sample collection, large sample volume and sterility make urine an ideal biofluid for high-throughput exploratory metabolomics to improve disease characterisation, diagnostics, disease monitoring, and treatment strategies. To this end, this study aimed to comprehensively characterise the urinary metabolic alterations in TB-T2DM patients in a South African population using untargeted ^{1}H-NMR metabolomics to identify potential mechanisms underlying interactions between TB and T2DM.

Materials and methods

Participants and sample collection

Voluntarily participating study participants were recruited from hospitals and community clinics situated in the Western Cape, South Africa, as part of the TANDEM study (48). The study cohort (n = 125) consisted of HCs with and without latent TB (n = 97) and TB-T2DM patients (n = 28). After considering further inclusion and exclusion criteria, a final cohort (n = 44) consisting of HCs (n = 15), HCs with latent TB (HCLTB; n = 15) and TB-T2DM patients (n = 14) was included in the analyses.

Individuals were excluded from the study if they were participating in a drug/vaccine trial, had other medical conditions such chronic bronchitis, asthma or emphysema requiring steroid therapy, cancer or a human immunodeficiency virus infection (current or within 3 months prior to enrolment), receiving steroid therapy within 6 months of enrolment, alcohol abuse (> 3 alcoholic beverages/day), participating in illicit drug use, were pregnant, lacking a physical address and/or not aged 18–70 years. The TB-T2DM group included only newly diagnosed TB cases confirmed by two independent positive sputum smears, positive Mycobacterium Growth Indicator Tube (MGIT) cultures, and/or positive polymerase chain reactions for bacterial DNA of the *Mtb* complex. Additionally, previously diagnosed (on T2DM treatment) or newly diagnosed T2DM with an HbA1c ≥ 6.5% (49) not induced by steroid therapy or pregnancy, also served as inclusion criteria for the TB-T2DM group. Individuals were excluded from the HC/HCLTB group if any of the following were present: an acute respiratory tract infection within four weeks prior to enrolment, prior/active T2DM or chronic hyperglycaemia, an active TB infection or any other systemic illnesses. Additionally, latent TB was confirmed by a positive QuantiFERON-Gold In-Tube assay (Qiagen, cat #622536), interpreted according to the manufacturer's specific cutoff values. Principal component analysis (PCA) and t-tests were performed on the HC group to determine whether latent TB influenced metabolic profiles. As no statistical differentiation was observed between participants with and without latent TB (**Fig. S1** in **Additional file 1**), these subgroups were combined into a single HC group (n = 30) to increase statistical power. The current study (Ethics number: NWU-00096-23-A1-02) falls under a larger study at the North-West University with the title: "The characterization of tuberculosis-diabetes mellitus co-morbidity in a South African cohort using metabolomics", for which ethics approval had been obtained (Ethics number: NWU-00096-23-A1). The clinical characteristics of the cohort are summarised in **Table 1**. The small TB-T2DM cohort size precluded stratification by T2DM duration, treatment type, or treatment duration.

Table 1: Clinical characteristics of the cohort consisting of healthy controls, healthy controls with latent TB, and TB-T2DM comorbid patients.

Clinical characteristic	Healthy controls (n = 15)	Healthy controls with latent TB (n = 15)	TB-T2DM (n = 14)
Sex (male/female)	5/10	7/8	7/7
Age in years (average ± standard deviation)	32.6 ± 10.45	45.4 ± 5.84	49.4 ± 6.37
HbA1c (%) (average ± standard deviation)	5.34 ± 0.43	5.33 ± 0.41	9.97 ± 2.1
T2DM (new/previously diagnosed)			4/10
Duration of T2DM (%)			
< 1 year			20
1–5 years			30
6–15 years			50
T2DM treatment (%)			
Insulin only			7.14
Metformin only			28.57
Metformin and other medications*			35.71
No medication			28.57
Duration of T2DM treatment (%) **			
< 1 year			20
15 years			30
6–15 years			50

HbA1c = percentage glycated haemoglobin
TB-T2DM = tuberculosis-type 2 diabetes mellitus
T2DM = type 2 diabetes mellitus
* = Includes one/more of the following: insulin, anti-hypertensive, statins, or other anti-DM medications.
** = Includes metformin and/or insulin and/or other T2DM medication as summarised in T2DM treatment.

Urine sample storage and transport

Study participants were asked to provide a urine sample in standard urine pots provided by the study nurses or clinicians, which were aliquoted and frozen at -80°C before being transported to the North-West University, where they were stored until ^{1}H-NMR analysis.

Reagents and chemicals

The reagents used for the NMR urine buffer preparation included: 3-(trimethylsilyl) propionic-2,2,3,3-d4 acid sodium salt (TSP) (CAS number: 24493-21-8), sodium azide (NaN_3) (CAS number: 26628-22-8), potassium dihydrogen phosphate (KH_2PO_4) (CAS number: 7778-77-0), potassium hydroxide (KOH) (CAS number: 1310-58-3), and deuterium oxide (D_2O) (CAS number: 7789-20-0). All reagents were purchased from Sigma Aldrich.

Urine buffer preparation

The NMR urine buffer was used to, amongst other things, maintain a constant pH of 7.4. The buffer contained an internal standard (TSP) to correct for analytical error, align the spectra, and quantify metabolites. The buffer was prepared as previously described (50). Briefly, 100 mg of TSP and 13 mg of the antimicrobial agent NaN_3 were dissolved in 10 mL of D_2O to give a final TSP concentration of 5.805 mM. Next, 20.4 g of KH_2PO_4 was dissolved in 80 mL of D_2O. Lastly, the two solutions were combined, the pH was adjusted to 7.4 with KOH pellets, and D_2O was added to a final volume of 100 mL.

Urine sample preparation

Firstly, a pooled quality control (QC) was prepared by aliquoting 80 µL from each sample into a single pooled QC, which was then split into two batches. The QCs were used to identify non-biological variation introduced by the environment, the analyst, or the analytical instrument, and to assess any batch effects (51). Samples were randomised into two batches, with a QC sample being analysed at the beginning, middle, and end of each batch. Urine sample preparation and ^{1}H-NMR analysis followed the same steps as described by Davoren and Mason (50). Briefly, 1000 µL of urine was centrifuged at 12,000 x *g* for 5 min in a micro-centrifuge tube to remove proteins or macromolecules that would lead to a poor baseline. Next, 540 µL of the supernatant was added to 60 µL of urine buffer (10% buffer: 90% sample) in a microcentrifuge tube and vortexed for 10 s. After a final centrifugation step at 12,000 x *g* for 5 min to remove precipitants, 540 µL of the supernatant was transferred to a 5 mm glass NMR tube and capped.

^{1}H-NMR analysis

The ^{1}H-NMR analysis was carried out as described in detail (50). Briefly, randomised samples were loaded onto the SampleXpress autosampler and analysed on a Bruker Avance III HD 500 MHz NMR spectrometer with a 5 mm TXI inverse probe. The first sample was used to lock onto D_2O in the sample to correct for any magnetic drift that may occur during the analysis (52). The probe was also tuned to 500.133 MHz, and shimming was performed using the TSP signal to align the magnetic field (53). The signal from water was suppressed by applying a Nuclear Overhauser Effect Spectroscopy pre-saturation (NOESY-presat) pulse program. Each scan consisted of an 8 µs excitation pulse at 90, followed by a 4 s relaxation delay. A total of 128 scans were done per sample. The probe temperature was kept constant at 300 K.

Spectral processing and statistical analysis

After sample analysis, Bruker Topspin (version 3.5) was used for Fourier transformation, TSP peak calibration to 0.00 ppm, and adjustment of the phase and baseline of the ^{1}H-NMR spectra. The spectral resolution was assessed by measuring the width of the TSP peak at half its height (< 1 Hz indicated good resolution) and assessing the two satellite peaks of TSP (50). Bruker AMIX (version 3.9.14) was used to visualise and divide the spectrum into 500 spectral bins of 0.02 ppm width to reduce data complexity, mitigate peak shifting between samples, and enable peak integration (54). Microsoft Excel (2019) was used for data cleanup and pre-processing. First, the H_2O peak at 4.69–4.89 ppm was removed. Next, the limit of detection (LOD) was calculated as the average of the blank spectral region plus 3.3 times its standard deviation. Noise removal was performed by replacing any spectral bin with an area below the LOD with a zero value and by using a 50% zero filter. Three bins with a coefficient of variation of > 30% across all six QCs were removed as experimental artefacts. Traditionally, creatinine normalisation is used for urine samples to correct for the variation in hydration status in a cohort (50), but creatinine is highly dependent on age and sex, and can be influenced by kidney damage (55). Osmolality normalisation has been shown to be more suitable for correcting hydration status than creatinine (56). Osmolality, determined by an OsmolPro instrument, was used to normalise each sample using the formula adapted from Chetwynd *et al.* (57) by dividing each bin by the osmolality of that sample.

Two rounds of univariate and multivariate statistical analyses were carried out using MetaboAnalyst (version 6.0) and Microsoft Excel (2019) to identify significant bins/metabolites. Bins that showed significant variation between HCs and TB-T2DM were identified in round 1 and used to identify and quantify metabolites relative to TSP (described below). Secondly, these metabolites then underwent a second round of statistical analysis to compile the final list of significant metabolites (round 2). Pre-processed bin/metabolite data were used to calculate non-parametric Wilcoxon-rank t-tests, combined with the Benjamini-Hochberg correction for multiple testing and false discovery rate (58), along with Hedge's G effect size (59) and the Log2(fold change) (Log2(FC)). Next, square root transformation and Pareto scaling were applied to ensure a Gaussian distribution for multivariate analysis. An unsupervised PCA was used to visualise clustering or separation between the two groups. Supervised partial least squares-discriminant analysis (PLS-DA) was used to identify features that contributed significantly to the observed variation between the two groups, as indicated by their variable of importance in projection (VIP) values. Selection criteria were adapted from Bester *et al.* (58). Given that this study used an untargeted metabolomics approach to inform future studies using more targeted and sensitive techniques, less stringent feature-selection criteria were applied. Bins/metabolites were selected when conforming to any one of the following: adjusted p-value ≤ 0.05, Log2(FC) ≤ -0.6 or ≥ 0.58, Hedge's G ≥ 0.6 (medium effect size), and a VIP value ≥ 1.0

Metabolite identification and quantification

Using bins determined as significant, Bruker AMIX (V3.9.14) and CHENOMX NMR suite (V8.2) were used to identify metabolites by using pure compound spectral libraries. Metabolite quantification was adapted from Davoren and Mason (50). First, metabolites were normalised to TSP for the purpose of quantification and to correct for experimental error using the following equation:

$$\frac{I_{TSP}}{I_{metabolite}} = \frac{H^{+}_{TSP} C_{TSP}}{H^{+}_{metabolite} C_{metabolite}} \#$$

I_{TSP}, H^{+}_{TSP}, *and* C_{TSP} represent the TSP integral, number of protons corresponding to this peak, and TSP concentration, respectively. The same is true for the selected metabolite: $I_{metabolite}$, $H^{+}_{metabolite}$, and $C_{metabolite}$. The metabolite concentrations were then divided by the sample's osmolality (mOsmol/kg H_2O) to correct for urine dilution variation. This value was then multiplied by 1000 to give the final metabolite concentration (uM/mOsmol/kg H_2O).

Results

Quality control and batch effect

To determine if a possible batch effect existed, the spectral data from all experimental and QC samples were analysed using a PCA plot. The absence of a batch effect is evident in the tight clustering of the six pooled QC samples on the PCA in **Fig. 1**. The average coefficient of variance value across all bins for all six QC samples was 2.3 %, which is considered very good for an ^{1}H-NMR analysis (50).

Statistical analysis

Two TB-T2DM patients with very high glucose signals that distorted their spectra and that would skew results were excluded from the 14 TB-T2DM patients. The PCA plot (PERMANOVA p-value = 0.001 with 999 permutations) of the HC and TB-T2DM cohorts (**Fig. 2**) showed partial separation, despite substantial intragroup heterogeneity in TB-T2DM cohort clinical characteristics (**Table 1**). The intragroup homogeneity of the HC group, which also contained the HCLTB group, is evident in the tight clustering of samples within this group (**Fig. 2**).

In total, 318 bins were selected as conforming to any one of the three univariate criteria as previously mentioned. These bins were then used to identify and quantify 28 metabolites. These values were used for the second round of statistical analyses. Of these, 23 metabolites (**Fig. S2** in **Additional file 1)** were identified as significant. The PLS-DA model was constructed from the quantified metabolite data, which passed validation with $Q^2 = 0.65$, $R^2 = 0.76$, and a permutation p-value < 0.05, using 2000 permutations (**Fig. 3**), although only two metabolites had significant VIP values. The final list of significant metabolites, as well as their corresponding p-values, log2(FC), and Hedge's G effect sizes, etc., is summarised in **Table 2**, and the main metabolic pathways affected are illustrated in **Fig. 4**.

Table 2: Summary of the urinary metabolites that differ significantly between the healthy control and TB-T2DM groups.

Metabolite	Human Metabolome Database ID	Effect size (Hedge's G)	Adjusted p-value	log2(FC) (TB-T2DM/HC)	TB-T2DM average (star
D-Glucose*	HMDB0003345	1.764	6.72×10^{-5}	6.737	101.904 (102.873)
D-Mannose	HMDB0000169	1.619	9.91×10^{-5}	2.684	1.093 (1.004)
Sucrose	HMDB0000168	1.068	6.94×10^{-3}	0.911	1.444 (0.531)
Lactate	HMDB0000190	0.753	3.86×10^{-2}	0.689	1.87 (1.444)
Pyruvate	HMDB0000166	0.666	6.13×10^{-2}	0.976	2.198 (2.761)
L-Alanine	HMDB0000161	0.906	1.66×10^{-2}	0.624	1.48 (0.845)
L-Isoleucine	HMDB0000172	0.982	1.05×10^{-2}	0.984	0.089 (0.076)
L-Leucine	HMDB0013773	0.994	1.05×10^{-2}	1.124	0.467 (0.437)
L-Valine	HMDB0000172	1.089	6.94×10^{-3}	0.97	0.441 (0.334)
L-Tyrosine	HMDB0000171	0.769	3.64×10^{-2}	0.572	0.512 (0.294)
β-Hydroxybutyrate	HMDB0000428	0.637	7.07×10^{-2}	0.604	0.452 (0.248)
Citrate	HMDB0000094	0.728	4.17×10^{-2}	0.65	5.706 (4.726)
α-Ketoglutarate	HMDB0000208	0.852	2.14×10^{-2}	0.809	0.99 (0.788)
Fumarate	HMDB0000134	1.04	7.83×10^{-3}	1.828	0.08 (0.098)
Succinate	HMDB0000167	1.177	4.20×10^{-2}	0.995	0.501 (0.346)
Dimethylamine	HMDB0000087	0.739	4.06×10^{-2}	0.454	0.807 (0.401)
Methylamine	HMDB0000164	0.864	2.14×10^{-2}	0.65	0.324 (0.2)
Trimethylamine	HMDB0000169	0.911	1.66×10^{-2}	0.673	0.158 (0.094)
Trimethylamine-N-oxide*	HMDB0000170	1.697	6.72×10^{-5}	6.539	85.401 (89.45)
Choline	HMDB0000097	1.366	8.90×10^{-4}	0.998	0.429 (0.241)
L-Carnitine	HMDB0000062	1.081	6.94×10^{-3}	1.158	0.653 (0.508)
Creatinine	HMDB0000562	0.609	8.15×10^{-2}	0.467	23.685 (14.944)
Methylguanidine	HMDB0000165	0.847	2.14×10^{-2}	0.72	0.376 (0.266)

Discussion

Glycolysis and gluconeogenesis

Significantly increased concentrations of glucose and mannose were evident in the TB-T2DM patients (Table 2 and Fig. 4). Both hexose sugars enter the cell via insulin-dependent (61, 62) and, to a lesser extent, insulin-independent glucose transporters (63, 64). This is well in accordance with previous findings in TB (32) and extensive systematic reviews on T2DM metabolomics (65, 66). Hyperglycaemia is well defined (67, 68), induced by insulin resistance (IR), followed by pancreatic β-cell destruction and hypoinsulinaemia in advanced T2DM patients. Elevated systemic mannose has also been associated with IR, impaired glucose tolerance, and is considered a risk for developing T2DM (69–71). In TB patients, an increased production of the catecholamines epinephrine and norepinephrine (which regulate immune activation) (19, 72) compromises insulin signalling and release (73, 74), thereby attenuating glucose

and mannose uptake (75). Additionally, elevated epinephrine increases hepatic glucose output by upregulating gluconeogenesis and glycogenolysis and downregulating the synthesis of muscle glycogen (76, 77). Considering that the comorbid patients in this study have a long history of T2DM, with 50% having had T2DM for 6–15 years prior to developing TB (**Table 1)**, hypoinsulinaemia is likely, although this was not directly measured. Moreover, only 2 of the 14 TB-T2DM patients were on insulin treatment at the time of sample collection (**Table 1)**. Thus, the hyperglycaemic effect of elevated epinephrine associated with an *Mtb* infection would be accentuated in patients with TB and pre-existing T2DM, given their already low insulin signalling capacity and/or reduced systemic insulin availability. Hyperglycaemia is also a direct consequence of a diet high in carbohydrates, which is evident in elevated urinary sucrose detected in the comorbid patients when compared to HCs (Table 2), indicative of a diet high in carbohydrates (78).

Due to reduced glucose uptake, gluconeogenesis compensates by synthesising glucose in the liver from lactate produced by the muscle. As such, there is an increased flux through this pathway supported by the significantly increased excretion of pyruvate and lactate in TB-T2DM patients (Table 2 and Fig. 4). This is in accordance with previous reports in the serum of TB (32, 79) and T2DM patients (25, 27). Guasch-Ferré *et al.* (65) also reported that increased serum lactate levels significantly correlate with T2DM risk and IR. The production of lactate from pyruvate also ensures the production of NAD^+ required to maintain/restore the cellular NAD^+/NADH redox balance (81). Studies have demonstrated that *Mtb* infection also compromises the cellular redox balance (i.e., reduced NAD^+/NADH ratio) in immune cells (82). Similarly, the same occurs in T2DM (83, 84). Interestingly, Boesten *et al.* (85) showed NAD^+ depletion in lung tissue from diabetic mice. The previously mentioned study by Reinecke *et al.*(39) identified increased flux through the NAD^+ *de novo* synthesis and salvage pathways, thereby supporting the notion of a NAD^+/NADH imbalance in TB-T2DM patients compared with HCs.

Alanine is also used as a gluconeogenic substrate to produce glucose in the liver in response to reduced insulin signalling and hypoglycaemia (86). Alanine acts as a carrier for the nitrogen, released by muscle proteolysis, to the liver for urea formation and excretion (87). Moreover, T2DM is marked by increased muscle proteolysis due to decreased insulin signalling (88). As such, the systemic alanine concentration is elevated in patients with T2DM compared to their healthy counterparts (66) and is also considered a risk factor for developing T2DM (80), consistent with the elevated urinary alanine in TB-T2DM patients in our study (Table 2). On the contrary, however, a decrease in systemic alanine has been associated with *Mtb* infection (89). In accordance with this, Peng *et al.* (90) showed that *Mtb* infection resulted in the depletion of human and murine systemic alanine and intracellular alanine in infected macrophages, thereby compromising host antimicrobial capacity. This discrepancy in alanine metabolism in TB, T2DM, and TB-T2DM patients in this study may be attributable to T2DM disease severity. The T2DM disease duration and extremely high HbA1c values, similar to those of poorly controlled T2DM (34), despite anti-T2DM medication use in the comorbid patients (**Table 1**), indicates severe T2DM. Contrarily, TB was more recently diagnosed in these patients, who were all considered newly diagnosed. As a result, the more severe T2DM-related alanine increases likely overshadow the TB-related alanine reduction.

Amino acids and the TCA cycle

As expected, there were also significantly increased concentrations of the branched-chain amino acids (BCAAs – leucine, valine, and isoleucine) and tyrosine (Table 2 and Fig. 4), associated with muscle wasting in both TB and T2DM (91). Increased tyrosine concentrations have been reported in the serum and urine of T2DM (34, 66) and TB patients (36, 89). The accumulation of the tyrosine degradation end-product, fumarate (Table 2), would contribute to this elevation. Moreover, elevated BCAAs in the plasma/serum of both TB (89, 92) and T2DM patients (25, 27) have been widely reported and even associated with the risk of developing T2DM. In support of this, urinary BCAA catabolite excretion has been shown to be decreased in TB-T2DM urine (39), pointing to a metabolic block in the BCAA catabolic pathway and thereby contributing to the increased BCAA excretion in this cohort. However, Ding *et al.* (93) reported a decrease in serum leucine in mice, zebrafish, and humans infected with *Mtb*. This is most likely due to the increased metabolic rate and wasting in TB (94), where leucine catabolism for energy would, in advanced TB, exceed its release into circulation via proteolysis. In agreement with this, Yun *et al.* (95) reported decreased valine levels in patients with poorly controlled T2DM. Considering this, the BCAA dynamics in TB and T2DM patients are most likely associated with disease severity and degree of muscle wasting. BCAAs activate mammalian target of rapamycin complex 1 (mTORC1); therefore, this complex would be overactivated by the aforementioned elevated BCAAs, typically seen in T2DM (96). Moreover, *Mtb* has been shown to activate mTORC1 to prevent autophagy-mediated clearance in macrophages (97, 98). Thus, chronic mTORC1 overactivation in T2DM patients by BCAAs would compromise macrophage autophagy-mediated antimicrobial capacity and increase the risk of developing active TB. On the other hand, infection-induced cytokine activation of mTORC1 (99) compromises insulin signalling, thereby promoting IR and increasing T2DM risk (100, 101) in TB patients. Overall, the induction of mTORC1 by elevated BCAAs in TB increases the risk of developing T2DM, and vice versa; this hypothesis warrants further investigation.

Intricately linked to muscle wasting and amino acid catabolism is the TCA cycle. It supports rapid energy production from fatty acids and amino acids, especially when glycolysis fails to meet energy demands. Overall, the TCA cycle maintains the fine balance between catabolic and anabolic pathways. The previously mentioned decrease in the NAD^+/NADH ratio leads to the inhibition of the TCA cycle enzymes isocitrate dehydrogenase (IDH), α-ketoglutarate dehydrogenase (OGDH), and malate dehydrogenase (MDH), which depend on NAD^+ (102). Considering that IDH and OGDH are two of the key points of regulation strongly inhibited by NADH (102), this would cause a significant metabolic block at these points of the TCA cycle. This is then exacerbated by the influx of amino acid catabolites via α-ketoglutarate, succinate, and fumarate. This metabolic block is evident in the accumulation of citrate, α-ketoglutarate, succinate, and fumarate in TB-T2DM patients relative to HCs (Table 2). Elevated succinate and fumarate have been associated with both TB (103) and T2DM (33, 34). Succinate (104) and fumarate (105) are both well-known indirect activators of hypoxia-inducible factor–1 alpha (HIF-1α). Moreover, these two metabolites can also inhibit the α-ketoglutarate-dependent destabilisation of HIF-1α (106). Increased HIF-1α signalling is additionally associated with reduced insulin secretion and sensitivity (107, 108). Considering this, the increased succinate and fumarate observed in this study will thus compromise insulin signalling via HIF-1α activation in TB.

The interconversion of α-ketoglutarate and glutamate is vital in the amination reactions involved in both amino acid synthesis and catabolism. Glutamate-derived α-ketoglutarate also feeds into the TCA cycle to support energy production and anabolism. Considering the increased systemic glutamate/glutamine ratio in T2DM (95) and TB (93), an increased supply of α-ketoglutarate is expected and seen in both TB (103) and T2DM (33). Citrate plays a vital role in regulating the TCA cycle, fatty acid synthesis, and glycolysis (109). It has been shown to be elevated in T2DM urine compared to HCs (33, 34). This is also

linked to the IR-related increase in β-oxidation (110) and, therefore, the supply of acetyl-CoA for citrate production. On the other hand, citrate is decreased in the urine (36) and serum (32) of TB patients and declines with the progression from latent- to active- to drug-resistant TB (103). This points to a more pronounced downregulation of pyruvate entry into the TCA cycle for citrate production in TB than in T2DM. Lastly, the two main ketone bodies produced from β-oxidation, β-hydroxybutyrate and acetoacetate, can be interconverted for energy production or to maintain the NAD^+/NADH ratio, with β-hydroxybutyrate production producing NAD^+. Only β-hydroxybutyrate was detected and elevated in TB-T2DM patients (Table 2), but the acetoacetate concentration was most probably below the detection limit, potentially due to a major shift towards β-hydroxybutyrate production to favour NAD^+ production.

Gut microbial and one-carbon metabolism

One-carbon metabolism plays a fundamental role in methylation reactions that modify DNA and RNA, as well as in various anabolic reactions. This investigation showed significant elevations in the one-carbon metabolites choline, trimethylamine-N-oxide (TMAO), trimethylamine (TMA), dimethylamine (DMA), and methylamine (MA) in TB-T2DM patients relative to HCs (Table 2). TMAO showed both a large increase and practical (Hedge's G) significance and statistical significance (FDR value) and contributed significantly to the observed general metabolic perturbation (VIP value) (Table 2) in the TB-T2DM group. TMAO is synthesised in the liver from trimethylamine (TMA) produced from dietary choline in the gut by gut microbes (111), with ~ 95% of the TMAO produced/absorbed being rapidly excreted in the urine (112). TMA and TMAO can also be converted to DMA, which then converts to MA (111). Considering this, the significant changes in TMAO in TB-T2DM patients were not unexpected, given the previously reported gut microbiota dysbiosis in TB (113) and T2DM (114). This dysbiosis was further confirmed by Reinecke *et al.* (39), who reported decreased urinary excretion of gut microbial metabolism metabolites such as phenylacetylglutamine and indoxyl in TB-T2DM patients versus HCs. Further support for this is the increased urinary (34, 115) and serum/plasma choline and TMAO (116, 117) previously reported in T2DM, as well as the fact that both TMAO (118) and choline (119) have been associated with an increased risk of developing T2DM. Jia *et al.* (119) additionally indicated that elevated TMAO results from the T2DM diseased state, rather than being a cause, and Miao *et al.* (120) showed that IR upregulates TMAO synthesis from TMA by increasing the expression of the hepatic flavin-containing monooxygenase 3 (FMO3) enzyme. TMAO is known to induce pro-inflammatory pathways (121, 122), which can have long-term detrimental effects on infection control and prognosis in TB if overactivated (123). Moreover, increased flux through the choline-TMAO pathway has also been associated with the formation of foamy macrophages (124), which promotes long-term *Mtb* persistence (125). Increased choline concentrations have also been reported in the serum of TB patients (79) versus HCs, although Vrieling *et al.* (126) reported a reduction in serum choline in TB and, to a lesser extent, in TB-T2DM patients compared with HCs. This depletion of choline can be linked to an increased demand for its derivatives, including phosphocholine, which has immunomodulatory effects in macrophages, among others, during infection (127). Moreover, Al-Sulaiti *et al.* (128) also showed reduced plasma choline and TMAO in T2DM patients with confirmed IR. The discrepancy in both TB and T2DM may hence be associated with disease severity, but also the fact that TMAO and choline dynamics in the body are strongly influenced by the gut microbiome, diet, age, and sex (129), warranting further investigation.

The main source of urinary DMA is asymmetric dimethylarginine (ADMA), but diet (and the resulting TMA and TMAO) also contributes to this (130). Although DMA is a marker for systemic ADMA, which is linked to several diseases, it can only be accurately measured in instances where diet is tightly controlled (130). Additionally, a very small portion of DMA is converted to MA and excreted in the urine. Considering the above, it can be inferred that the significantly elevated TMAO and its upstream metabolites observed in TB-T2DM in this study are a result of advanced T2DM. However, more studies targeting this pathway in TB patients are needed to determine the contribution of TB to this metabolic profile in comorbid patients.

Carnitine

Similar to TMA and TMAO, the diet is the main source of carnitine, and it can also be converted to TMA in the gut (131). Carnitine showed a greater urinary excretion in comorbid patients relative to HCs (Table 2) in accordance with decreased renal carnitine reabsorption in diabetes (132) and systemic carnitine deficiencies in both diabetes (132) and TB (133). Considering that carnitine plays an important role in improving T-cell bactericidal function, as confirmed in TB patients (134, 135), the diabetes-related deficiency would promote *Mtb* proliferation. Additionally, IR associated with T2DM would lead to an increased consumption of carnitine to produce acylcarnitines via carnitine palmitoyl transferase 1 (CPT1) (136).

Creatinine pathway

Creatinine and methylguanidine were increased in TB-T2DM comparatively (Table 2). Although increased creatinine excretion has been directly associated with muscle mass/muscle breakdown (137), it is also used as a marker for kidney damage (55) and T2DM (33, 138). Despite the strong effects of diet, age, sex, and hydration status on creatinine excretion (139) and the significant heterogeneity in the TB-T2DM group (**Table 1** and **Fig. 2**), creatinine remained significant. Creatinine can also non-enzymatically be oxidised to methylguanidine, a well-known uremic toxin in patients with renal failure (140) and associated with poorly controlled diabetes (141).

The results of this study are distinct from, yet complementary to, the previously mentioned findings of Reinecke *et al.* (39) that identified significant alterations in nucleotide salvage, the kynurenine pathway, NAD^+ synthesis and salvage, tyrosine metabolism, lipid oxidation and glycine conjugation. Other than BCAAs, our study did not identify metabolites directly linked to these pathways. This is due to the use of different analytical platforms, which affect sensitivity, accuracy, and potential bias toward polar or non-polar metabolites. Nonetheless, the metabolic block in BCAA catabolism and NAD^+/NADH imbalance in TB-T2DM patients are supported by both studies.

Conclusion

This ^{1}H-NMR metabolomic analysis characterised metabolic profiles in TB-T2DM patients, uncovering potential metabolic mechanisms underlying the interaction between TB and T2DM. However, most metabolic alterations mirror those observed in TB and/or T2DM, suggesting a synergistic interaction between the two. Overall, Epinephrine production in TB promotes IR, hypoinsulinaemia and glucose production, thereby exacerbating both hyperglycaemia and T2DM risk and severity. Similarly, increased alanine (gluconeogenic flux) in TB-T2DM is associated with severe T2DM, with a lesser contribution from TB-

related alanine depletion to this profile. mTORC1 overactivation due to increased BCAAs in TB and T2DM leads to IR, promoting T2DM, and compromised macrophage antimicrobial capacity, promoting TB. The significant NAD^+/NADH imbalance inferred from alterations in the lactate, TCA cycle, and BCAA pathways necessitates more direct measurements to assess disease interactions and the diagnostic potential of these pathways. Furthermore, the NAD^+/NADH imbalance and amino acid catabolism related to succinate and fumarate accumulation in TB reduce insulin secretion and sensitivity via HIF-1α. The expected alterations in one-carbon gut microbial metabolism are highlighted as playing causal and reverse-causal roles in both TB and T2DM, meriting tissue-specific targeting of this pathway. This study also identified markers of kidney damage, namely creatinine and methylguanidine, and potential systemic carnitine deficiencies. Although less common, it remains unclear how severe TB interacts with less severe T2DM (transient hyperglycaemia excluded), a question that merits further investigation.

Limitations

Variation in clinical characteristics, such as disease duration/severity, differences in treatment, age and sex distribution, and the small sample size after applying exclusion criteria, inherent to a study of this kind, may introduce bias that can be avoided when using a larger cohort. However, the distinct metabolic profile observed in TB-T2DM patients compared to HCs, as well as the natural separation identified by multivariate statistics, indicate that, despite the possible variation/bias, the severe diseased state still induces significant metabolic alterations, despite the small sample size.

Abbreviations

PLS-DA Partial least squares–discriminant analysis

PCA Principal component analysis

Log2(FC) Log2(fold change)

TB Tuberculosis

T2DM Type 2 diabetes mellitus

TB-T2DM Tuberculosis-type 2 diabetes mellitus comorbidity

^{1}H-NMR Proton nuclear magnetic resonance spectroscopy

Mtb Mycobacterium tuberculosis

HC Healthy control

HbA1c Glycated haemoglobin

IR Insulin resistance

NAD^+ Nicotinamide adenine dinucleotide (oxidised)

NADH Nicotinamide adenine dinucleotide (reduced)

BCAA Branched-chain amino acid

mTORC1 Mammalian target of rapamycin complex 1

HIF-1α Hypoxia-inducible factor-1α

TMAO Trimethylamine-N-oxide

TCA Tricarboxylic acid

TSP Trimethylsilylpropanoic acid

VIP Variable importance in projection

GCxGC-TOFMS Two-dimensional gas chromatography coupled to time-of-flight mass spectrometry

Declarations

Ethics approval

All procedures carried out in this study were approved by the Stellenbosch University Health Research Ethics Committee (ethics reference number: N13/05/064; project ID: 4095) and the North-West University Health Research Ethics Committee (ethics reference number: NWU-00096-23-A1). All procedures were carried out in accordance with the Declaration of Helsinki.

Consent to participate

Participation in the study was entirely voluntary. After being fully informed about the study all participants gave informed consent to the use of their samples and de-identified clinical data.

Consent for publication

Not applicable.

Clinical trial number

Not applicable

Availability of data and materials

The datasets used and/or analysed during the current study are available from the corresponding author on reasonable request.

Competing interests

The authors declare that they have no competing interests.

Funding

This work was supported by funding from the National Research Foundation (NRF) of South Africa [grant number: SRUG2204062208]. The opinions, findings, and conclusions or recommendations expressed are those of the authors alone, and the NRF accepts no liability.

Author contributions

The design for the original research study was conceptualised and designed by DTL. The samples were collected and supplied by LK and KR. ST prepared and analysed the urine samples and performed the data processing. SM advised ST on sample analysis and data processing. ST and DTL interpreted the results. The manuscript was written by ST and edited by DTL and SM. All authors read and approved the final manuscript.

Acknowledgments

Not applicable

References

1. World Health Organisation (WHO). Global Tuberculosis Report 2024. 2024. Available online: https://www.who.int/publications/m/item/top-findings-and-messages-in-the-2024-report
2. International Diabetes Federation (IDF). IDF Diabetes Atlas 2025. 2025. Report No.: 978-2-930229-96-6.
3. Li M, Chen T, Hua Z, Yan H, Wang D, Li Z, et al. Global, regional, and national prevalence of diabetes mellitus in patients with pulmonary tuberculosis: a systematic review and meta-analysis. Diabetol Metab Synd. 2021;13(1):127.
4. Workneh MH, Bjune GA, Yimer SA. Prevalence and associated factors of tuberculosis and diabetes mellitus comorbidity: A systematic review. PLoS One. 2017;12(4):e0175925.
5. Damtie S, Legese B, Fentie A, Solomon Y, Erkihun M, Molla T, et al. Diabetes mellitus and its determinants among tuberculosis patients in South Gondar Zone health facilities, Northwest Ethiopia. Sci Rep. 2025;15(1):5813.
6. Glaziou P, Floyd K, Raviglione MC. Global epidemiology of tuberculosis. Semin Respir Crit Care Med. 2018;39(03):271–85.
7. Behr MA, Kaufmann E, Duffin J, Edelstein PH, Ramakrishnan L. Latent tuberculosis: Two centuries of confusion. Am J Respir Crit Care Med. 2021;204(2):142–8.
8. Narasimhan P, Wood J, Macintyre CR, Mathai D. Risk factors for tuberculosis. Pulm Med. 2013;2013:828939.
9. Hensel RL, Kempker RR, Tapia J, Oladele A, Blumberg HM, Magee MJ. Increased risk of latent tuberculous infection among persons with pre-diabetes and diabetes mellitus. Int J Tuberc Lung Dis. 2016;20(1):71–8.
10. Baker MA, Harries AD, Jeon CY, Hart JE, Kapur A, Lönnroth K, et al. The impact of diabetes on tuberculosis treatment outcomes: A systematic review. BMC Med. 2011;9(1):81.
11. Jeon CY, Murray MB. Diabetes mellitus increases the risk of active tuberculosis: A systematic review of 13 observational studies. PLoS Med. 2008;5(7):e152.
12. Lee PH, Fu H, Lai TC, Chiang CY, Chan CC, Lin HH. Glycemic control and the risk of tuberculosis: A cohort study. PLoS Med. 2016;13(8):e1002072.
13. Evangelista MdSN, Maia R, Toledo JP, Abreu RGd, Barreira D. Tuberculosis associated with diabetes mellitus by age group in Brazil: A retrospective cohort study, 2007–2014. Braz J Infect Dis. 2020;24(2):130–6.
14. Chatterjee S, Khunti K, Davies MJ. Type 2 diabetes. Lancet. 2017;389(10085):2239–51.
15. Atkinson MA, Eisenbarth GS, Michels AW. Type 1 diabetes. Lancet. 2014;383(9911):69–82.
16. Dooley KE, Chaisson RE. Tuberculosis and diabetes mellitus: Convergence of two epidemics. Lancet Infect Dis. 2009;9(12):737–46.

17. Meregildo-Rodriguez ED, Asmat-Rubio MG, Zavaleta-Alaya P, Vásquez-Tirado GA. Effect of oral antidiabetic drugs on tuberculosis risk and treatment outcomes: Systematic review and meta-analysis. Trop Med Infect Dis. 2022;7(11):343.
18. Wishart DS. Metabolomics for investigating physiological and pathophysiological processes. Physiol Rev. 2019;99(4):1819–75.
19. du Preez I, Loots DT. New sputum metabolite markers implicating adaptations of the host to *Mycobacterium tuberculosis*, and vice versa. Tuberculosis. 2013;93(3):330–7.
20. Collins JM, Siddiqa A, Jones DP, Liu K, Kempker RR, Nizam A, et al. Tryptophan catabolism reflects disease activity in human tuberculosis. JCI Insight. 2020;5(10):e137131.
21. Weiner J, 3rd, Maertzdorf J, Sutherland JS, Duffy FJ, Thompson E, Suliman S, et al. Metabolite changes in blood predict the onset of tuberculosis. Nat Commun. 2018;9(1):5208.
22. Das MK, Bishwal SC, Das A, Dabral D, Badireddy VK, Pandit B, et al. Deregulated tyrosine-phenylalanine metabolism in pulmonary tuberculosis patients. J Proteome Res. 2015;14(4):1947–56.
23. Das MK, Savidge B, Pearl JE, Yates T, Miles G, Pareek M, et al. Altered hepatic metabolic landscape and insulin sensitivity in response to pulmonary tuberculosis. PLoS Pathog. 2024;20(9):e1012565.
24. Rebholz C, Yu B, Zheng Z, Chang P, Tin A, Köttgen A, et al. Serum metabolomic profile of incident diabetes. Diabetologia. 2018;61(5):1046–54.
25. Nokhoijav E, Guba A, Kumar A, Kunkli B, Kalló G, Káplár M, et al. Metabolomic analysis of serum and tear samples from patients with obesity and type 2 diabetes mellitus. Int J Mol Sci. 2022;23(9):4534.
26. Salihovic S, Broeckling CD, Ganna A, Prenni JE, Sundström J, Berne C, et al. Non-targeted urine metabolomics and associations with prevalent and incident type 2 diabetes. Sci Rep. 2020;10(1):16474.
27. Sharma S, Dong Q, Haid M, Adam J, Bizzotto R, Fernandez-Tajes JJ, et al. Role of human plasma metabolites in prediabetes and type 2 diabetes from the IMI-DIRECT study. Diabetologia. 2024;67(12):2804–18.
28. Taya N, Katakami N, Omori K, Arakawa S, Hosoe S, Watanabe H, et al. Evaluation of change in metabolome caused by comprehensive diabetes treatment: A prospective observational study of diabetes inpatients with GC/MS-based non-target metabolomic analysis. J Diabetes Investig. 2021;12:2232–41.
29. Palmer ND, Stevens RD, Antinozzi PA, Anderson A, Bergman RN, Wagenknecht LE, et al. Metabolomic profile associated with insulin resistance and conversion to diabetes in the Insulin Resistance Atherosclerosis Study. J Clin Endocrinol Metab. 2015;100(3):E463–8.
30. Drábková P, Šanderová J, Kovařík J, KanĎár R. An assay of selected serum amino acids in patients with type 2 diabetes mellitus. Adv Clin Exp Med. 2015;24(3):447–51.
31. Cho Y, Park Y, Sim B, Kim J, Lee H, Cho SN, et al. Identification of serum biomarkers for active pulmonary tuberculosis using a targeted metabolomics approach. Sci Rep. 2020;10(1):3825.
32. Conde R, Laires R, Goncalves LG, Rizvi A, Barroso C, Villar M, et al. Discovery of serum biomarkers for diagnosis of tuberculosis by NMR metabolomics including cross-validation with a second cohort. Biomed J. 2022;45(4):654–64.
33. Guan M, Xie L, Diao C, Wang N, Hu W, Zheng Y, et al. Systemic Perturbations of key metabolites in diabetic rats during the evolution of diabetes studied by urine netabonomics. PLoS One. 2013;8(4):e60409.
34. Theron IJ, Mason S, van Reenen M, Stander Z, Kleynhans L, Ronacher K, et al. Characterizing poorly controlled type 2 diabetes using (1)H-NMR metabolomics. Metabolomics. 2024;20(3):54.
35. Luier L, Loots DT. Tuberculosis metabolomics reveals adaptations of man and microbe in order to outcompete and survive. Metabolomics. 2016;12(3):40.
36. Olivier C, Luies L. Metabolic insights into HIV/TB co-infection: An untargeted urinary metabolomics approach. Metabolomics. 2024;20(4):78.
37. Vrieling F, Alisjahbana B, Sahiratmadja E, Van Crevel R, Harms A, Hankemeier T, et al. Plasma metabolomics in tuberculosis patients with and without concurrent type 2 diabetes at diagnosis and during antibiotic treatment. Sci Rep. 2019;9:18669.
38. Vrieling F, Ronacher K, Kleynhans L, van den akker E, Walzl G, Ottenhoff T, et al. Patients with concurrent tuberculosis and diabetes have a pro-atherogenic plasma lipid profile. EBioMedicine. 2018;32:192–200.
39. Reinecke K, Kleynhans L, Ronacher K, Loots DT. Characterizing the tuberculosis and type 2 diabetes mellitus comorbidity in a South African cohort using untargeted GCxGC-TOFMS metabolomics. Metabolomics. 2026;22(1):19.
40. Büscher JM, Czernik D, Ewald JC, Sauer U, Zamboni N. Cross-platform comparison of methods for quantitative metabolomics of primary metabolism. Anal Chem. 2009;81(6):2135–43.
41. Savorani F, Rasmussen MA, Mikkelsen MS, Engelsen SB. A primer to nutritional metabolomics by NMR spectroscopy and chemometrics. Food Res Int. 2013;54(1):1131–45.
42. González-Domínguez R, González-Domínguez Á, Sayago A, Fernández-Recamales Á. Recommendations and best practices for standardizing the pre-analytical processing of blood and urine samples in metabolomics. Metabolites. 2020;10(6):229.
43. Dunn WB, Ellis DI. Metabolomics: Current analytical platforms and methodologies. Trends Anal Chem. 2005;24(4):285–94.
44. Li T, Ihanus A, Ohukainen P, Järvelin M-R, Kähönen M, Kettunen J, et al. Clinical and biochemical associations of urinary metabolites: Quantitative epidemiological approach on renal-cardiometabolic biomarkers. Int J Epidemiol. 2023;53(1):dyad162.
45. Zhang Z, Liu J, Cheng Y, Chen J, Zhao H, Ren X. Urine analysis has a very broad prospect in the future. Front Anal Sci. 2022;1:812301.

46. Li Z, Zhang Y, Hoene M, Fritsche L, Zheng S, Birkenfeld A, et al. Diagnostic performance of sex-specific modified metabolite patterns in urine for screening of prediabetes. Front Endocrinol. 2022;13:935016.
47. Yousri NA, Mook-Kanamori DO, Selim MM, Takiddin AH, Al-Homsi H, Al-Mahmoud KA, et al. A systems view of type 2 diabetes-associated metabolic perturbations in saliva, blood and urine at different timescales of glycaemic control. Diabetologia. 2015;58(8):1855–67.
48. van Crevel R, Dockrell HM. TANDEM: Understanding diabetes and tuberculosis. Lancet Diabetes Endocrinol. 2014;2(4):270–2.
49. American Diabetes Association Professional Practice Committee (ADAPP). Diagnosis and classification of diabetes: Standards of care in diabetes—2026. Diabetes Care. 2026;48(Supplement_1):S27–49.
50. Davoren E, Mason S. (1)H-NMR protocol for rapid diagnosis of purine and pyrimidine metabolic disorders in urine. STAR Protoc. 2023;4(2):102181.
51. Broeckling CD, Beger RD, Cheng LL, Cumeras R, Cuthbertson DJ, Dasari S, et al. Current practices in LC-MS untargeted metabolomics: A scoping review on the use of pooled quality control samples. Anal Chem. 2023;95(51):18645–54.
52. Haslauer KE, Hemmler D, Schmitt-Kopplin P, Heinzmann SS. Guidelines for the use of deuterium oxide (D_2O) in ^1H NMR metabolomics. Anal Chem. 2019;91(17):11063–9.
53. Fuks LF, Huang FSC, Carter CM, Edelstein WA, Roemer PB. Susceptibility, lineshape, and shimming in high-resolution NMR. J Magn Reson. 1992;100(2):229–42.
54. Chai X, Liu C, Fan X, Huang T, Zhang X, Jiang B, et al. Combination of peak-picking and binning for NMR-based untargeted metabonomics study. J Magn Reso. 2023;351:107429.
55. Butt B, Ghulam B, Bashir Z, Abbasi SR, Hussain S, Jadoon SK, et al. Enhanced creatinine level in diabetic patients maximizing the possibilities of nephropathy and its association with blood urea nitrogen and glomerular filtration rate. Cureus. 2024;16(9):e70482.
56. Mervant L, Tremblay-Franco M, Jamin EL, Kesse-Guyot E, Galan P, Martin JF, et al. Osmolality-based normalization enhances statistical discrimination of untargeted metabolomic urine analysis: Results from a comparative study. Metabolomics. 2021;17(1):2.
57. Chetwynd AJ, Abdul-Sada A, Holt SG, Hill EM. Use of a pre-analysis osmolality normalisation method to correct for variable urine concentrations and for improved metabolomic analyses. J Chromatogr A. 2016;1431:103–10.
58. Jafari M, Ansari-Pour N. Why, when and how to adjust your p values? Cell J. 2018;20(4):604–7.
59. Ialongo C. Understanding the effect size and its measures. Biochem Med. 2016;26(2):150–63.
60. Bester R, Stander Z, Mason S, Keane KM, Howatson G, Clifford T, et al. Characterizing marathon-induced metabolic changes using 1H-NMR metabolomics. Metabolites. 2021;11(10):656.
61. Ryder JW, Kawano Y, Chibalin AV, Rincón J, Tsao TS, Stenbit AE, et al. In vitro analysis of the glucose-transport system in GLUT4-null skeletal muscle. Biochem J. 1999;342(Pt 2):321–8.
62. Ryder JW, Yang J, Galuska D, Rincón J, Björnholm M, Krook A, et al. Use of a novel impermeable biotinylated photolabeling reagent to assess insulin- and hypoxia-stimulated cell surface GLUT4 content in skeletal muscle from type 2 diabetic patients. Diabetes. 2000;49(4):647–54.
63. Koumanov F, Yang J, Jones AE, Hatanaka Y, Holman GD. Cell-surface biotinylation of GLUT4 using bis-mannose photolabels. Biochem J. 1998;330(Pt 3):1209–15.
64. Hulett NA, Scalzo RL, Reusch JEB. Glucose uptake by skeletal muscle within the contexts of type 2 diabetes and exercise: An integrated approach. Nutrients. 2022;14(3):647.
65. Guasch-Ferré M, Hruby A, Toledo E, Clish CB, Martínez-González MA, Salas-Salvadó J, et al. Metabolomics in prediabetes and diabetes: A systematic review and meta-analysis. Diabetes Care. 2016;39(5):833–46.
66. Morze J, Wittenbecher C, Schwingshackl L, Danielewicz A, Rynkiewicz A, Hu FB, et al. Metabolomics and type 2 diabetes risk: An updated systematic review and meta-analysis of prospective cohort studies. Diabetes Care. 2022;45(4):1013–24.
67. Cerf ME. Beta cell dysfunction and insulin resistance. Front Endocrinol. 2013;4:37.
68. Hudish LI, Reusch JEB, Sussel L. β Cell dysfunction during progression of metabolic syndrome to type 2 diabetes. J Clin Investig. 2019;129(10):4001–8.
69. Lee S, Zhang C, Kilicarslan M, Piening Brian D, Bjornson E, Hallström Björn M, et al. Integrated network analysis reveals an association between plasma mannose levels and insulin resistance. Cell Metab. 2016;24(1):172–84.
70. Amano E, Funakoshi S, Yoshimura K, Hirano S, Ohmi S, Takata H, et al. Fasting plasma mannose levels are associated with insulin sensitivity independent of BMI in Japanese individuals with diabetes. Diabetol Metab Syndr. 2018;10:88.
71. Fortin E, Campi B, Ferrannini E, Mari A, Mellbin LG, Norhammar A, et al. High mannose correlates with surrogate indexes of insulin resistance and is associated with an increased risk of cardiovascular events independently of glycemic status and traditional risk factors. Diabetes Care. 2023;47(2):246–51.
72. Thoppil J, Mehta P, Bartels B, Sharma D, Farrar JD. Impact of norepinephrine on immunity and oxidative metabolism in sepsis. Front Immunol. 2023;14:1271098.
73. Viguerie N, Clement K, Barbe P, Courtine M, Benis A, Larrouy D, et al. In vivo epinephrine-mediated regulation of gene expression in human skeletal muscle. J Clin Endocrinol Metab. 2004;89(5):2000–14.
74. Sluga N, Križančić Bombek L, Kerčmar J, Sarikas S, Postić S, Pfabe J, et al. Physiological levels of adrenaline fail to stop pancreatic beta cell activity at unphysiologically high glucose levels. Front Endocrinol. 2022;13:1013697.
75. Watt MJ, Hargreaves M. Effect of epinephrine on glucose disposal during exercise in humans: Role of muscle glycogen. Am J Physiol-Endocrinol Metab. 2002;283(3):E578–83.

76. McGuinness OP, Shau V, Benson EM, Lewis M, Snowden RT, Greene JE, et al. Role of epinephrine and norepinephrine in the metabolic response to stress hormone infusion in the conscious dog. American Journal of Physiology-Endocrinology and Metabolism. 1997;273(4):E674–81.
77. Jensen J, Ruge T, Lai Y-C, Svensson MK, Eriksson JW. Effects of adrenaline on whole-body glucose metabolism and insulin-mediated regulation of glycogen synthase and PKB phosphorylation in human skeletal muscle. Metab - Clin Exp. 2011;60(2):215–26.
78. Tasevska N, Runswick SA, McTaggart A, Bingham SA. Urinary sucrose and fructose as biomarkers for sugar consumption. Cancer Epidemiol Biomarkers Prev. 2005;14(5):1287–94.
79. Albors-Vaquer A, Rizvi A, Matzapetakis M, Lamosa P, Coelho AV, Patel AB, et al. Active and prospective latent tuberculosis are associated with different metabolomic profiles: clinical potential for the identification of rapid and non-invasive biomarkers. Emerg Microbes Infect. 2020;9(1):1131–9.
80. Guasch-Ferré M, Santos JL, Martínez-González MA, Clish CB, Razquin C, Wang D, et al. Glycolysis/gluconeogenesis- and tricarboxylic acid cycle–related metabolites, Mediterranean diet, and type 2 diabetes. Am J Clin Nutr. 2020;111(4):835–44.
81. Lagarde D, Jeanson Y, Portais JC, Galinier A, Ader I, Casteilla L, et al. Lactate fluxes and plasticity of adipose tissues: A redox perspective. Front Physiol. 2021;12:689747.
82. Pajuelo D, Gonzalez-Juarbe N, Tak U, Sun J, Orihuela CJ, Niederweis M. NAD(+) depletion triggers macrophage necroptosis, a cell death pathway exploited by *Mycobacterium tuberculosis*. Cell Rep. 2018;24(2):429–40.
83. Chiao YA, Chakraborty AD, Light CM, Tian R, Sadoshima J, Shi X, et al. NAD^+ redox imbalance in the heart exacerbates diabetic cardiomyopathy. Circ: Heart Fail. 2021;14(8):e008170.
84. Wu J, Jin Z, Yan LJ. Redox imbalance and mitochondrial abnormalities in the diabetic lung. Redox Biol. 2017;11:51–9.
85. Boesten DMPHJ, von Ungern-Sternberg SNI, den Hartog GJM, Bast A. Protective pleiotropic effect of flavonoids on NAD+ levels in endothelial cells exposed to high glucose. Oxid Med Cell Longev. 2015;2015(1):894597.
86. Sahoo B, Srivastava M, Katiyar A, Ecelbarger C, Tiwari S. Liver or kidney: Who has the oar in the gluconeogenesis boat and when? World J Diabetes. 2023;14(7):1049–56.
87. Sarabhai T, Roden M. Hungry for your alanine: When liver depends on muscle proteolysis. J Clin Invest. 2019;129(11):4563–6.
88. James HA, O'Neill BT, Nair KS. Insulin regulation of proteostasis and clinical implications. Cell Metab. 2017;26(2):310–23.
89. Zhou A, Ni J, Xu Z, Wang Y, Lu S, Sha W, et al. Application of (1)h NMR spectroscopy-based metabolomics to sera of tuberculosis patients. J Proteome Res. 2013;12(10):4642–9.
90. Peng C, Cheng Y, Ma M, Chen Q, Duan Y, Liu S, et al. *Mycobacterium tuberculosis* suppresses host antimicrobial peptides by dehydrogenating L-alanine. Nature Commun. 2024;15(1):4216.
91. Ferrer M, Anthony TG, Ayres JS, Biffi G, Brown JC, Caan BJ, et al. Cachexia: A systemic consequence of progressive, unresolved disease. Cell. 2023;186(9):1824–45.
92. Shin J-H, Yang J-Y, Jeon B-Y, Yoon YJ, Cho S-N, Kang Y-H, et al. 1H NMR-based metabolomic profiling in mice infected with *Mycobacterium tuberculosis*. J Proteome Res. 2011;10(5):2238–47.
93. Ding Y, Raterink RJ, Marin-Juez R, Veneman WJ, Egbers K, van den Eeden S, et al. Tuberculosis causes highly conserved metabolic changes in human patients, mycobacteria-infected mice and zebrafish larvae. Sci Rep. 2020;10(1):11635.
94. Chang SW, Pan WS, Lozano Beltran D, Oleyda Baldelomar L, Solano MA, Tuero I, et al. Gut hormones, appetite suppression and cachexia in patients with pulmonary TB. PLoS One. 2013;8(1):e54564.
95. Yun JH, Lee HS, Yu HY, Kim YJ, Jeon HJ, Oh T, et al. Metabolomics profiles associated with HbA1c levels in patients with type 2 diabetes. PLoS One. 2019;14(11):e0224274.
96. Zhenyukh O, Civantos E, Ruiz-Ortega M, Sánchez MS, Vázquez C, Peiró C, et al. High concentration of branched-chain amino acids promotes oxidative stress, inflammation and migration of human peripheral blood mononuclear cells via mTORC1 activation. Free Radic Biol Med. 2017;104:165–77.
97. Quadir N, Shariq M, Sheikh JA, Singh J, Sharma N, Hasnain SE, et al. *Mycobacterium tuberculosis* protein MoxR1 enhances virulence by inhibiting host cell death pathways and disrupting cellular bioenergetics. Virulence. 2023;14(1):2180230.
98. Duan L, Yi M, Chen J, Li S, Chen W. *Mycobacterium tuberculosis* EIS gene inhibits macrophage autophagy through up-regulation of IL-10 by increasing the acetylation of histone H3. Biochem Biophys Res Commun. 2016;473(4):1229–34.
99. Wang H, Li J, Han Q, Yang F, Xiao Y, Xiao M, et al. IL-12 influence mTOR to modulate CD8(+) T cells differentiation through T-bet and eomesodermin in response to invasive pulmonary aspergillosis. Int J Med Sci. 2017;14(10):977–83.
100. Amin NG, Rahim AA, Rohoma K, Elwafa RAA, Dabees HMF, Elrahmany S. The relation of mTOR with diabetic complications and insulin resistance in patients with type 2 diabetes mellitus. Diabetol Metab Syndr. 2024;16(1):222.
101. Shah OJ, Wang Z, Hunter T. Inappropriate activation of the TSC/Rheb/mTOR/S6K cassette induces IRS1/2 depletion, insulin resistance, and cell survival deficiencies. Curr Biol. 2004;14(18):1650–6.
102. Arnold PK, Finley LWS. Regulation and function of the mammalian tricarboxylic acid cycle. J Biol Chem. 2023;299(2):102838.
103. Collins JM, Jones DP, Sharma A, Khadka M, Liu KH, Kempker RR, et al. TCA cycle remodeling drives proinflammatory signaling in humans with pulmonary tuberculosis. PLoS Pathog. 2021;17(9):e1009941.
104. Xu J, Zheng Y, Zhao Y, Zhang Y, Li H, Zhang A, et al. Succinate/IL-1β signaling axis promotes the inflammatory progression of endothelial and exacerbates atherosclerosis. Front Immunol. 2022;13:817572.

105. Isaacs JS, Jung YJ, Mole DR, Lee S, Torres-Cabala C, Chung YL, et al. HIF overexpression correlates with biallelic loss of fumarate hydratase in renal cancer: Novel role of fumarate in regulation of HIF stability. Cancer Cell. 2005;8(2):143–53.
106. Xiao M, Yang H, Xu W, Ma S, Lin H, Zhu H, et al. Inhibition of α-KG-dependent histone and DNA demethylases by fumarate and succinate that are accumulated in mutations of FH and SDH tumor suppressors. Genes Dev. 2012;26(12):1326–38.
107. Kihira Y, Miyake M, Hirata M, Hoshina Y, Kato K, Shirakawa H, et al. Deletion of hypoxia-inducible factor-1α in adipocytes enhances glucagon-like peptide-1 secretion and reduces adipose tissue inflammation. PLoS One. 2014;9(4):e93856.
108. Jiang C, Qu A, Matsubara T, Chanturiya T, Jou W, Gavrilova O, et al. Disruption of hypoxia-inducible factor 1 in adipocytes improves insulin sensitivity and decreases adiposity in high-fat diet–fed mice. Diabetes. 2011;60(10):2484–95.
109. Westergaard N, Waagepetersen HS, Belhage B, Schousboe A. Citrate, a ubiquitous key metabolite with regulatory function in the CNS. Neurochem Res. 2017;42(6):1583–8.
110. Abel ED. Free fatty acid oxidation in insulin resistance and obesity. Heart Metab. 2010;48:5–10.
111. Gatarek P, Kaluzna-Czaplinska J. Trimethylamine N-oxide (TMAO) in human health. Excli J. 2021;20:301–19.
112. Al-waiz M, Mitchell SC, Idle JR, Smith RL. The metabolism of 14C-labelled trimethylamine and its N-oxide in man. Xenobiotica. 1987;17(5):551–8.
113. Han M, Wang X, Zhang J, Su L, Ishaq HM, Li D, et al. Gut bacterial and fungal dysbiosis in tuberculosis patients. BMC Microbiol. 2024;24(1):141.
114. Neri-Rosario D, Martínez-López YE, Esquivel-Hernández DA, Sánchez-Castañeda JP, Padron-Manrique C, Vázquez-Jiménez A, et al. Dysbiosis signatures of gut microbiota and the progression of type 2 diabetes: A machine learning approach in a Mexican cohort. Front Endocrinol. 2023;14:1170459.
115. Messana I, Forni F, Ferrari F, Rossi C, Giardina B, Zuppi C. Proton nuclear magnetic resonance spectral profiles of urine in type II diabetic patients. Clin Chem. 1998;44(7):1529–34.
116. Kalagi NA, Thota RN, Stojanovski E, Alburikan KA, Garg ML. Association between plasma trimethylamine N-oxide levels and type 2 diabetes: A case control study. Nutrients. 2022;14(10):2093.
117. Zeng Q, Zhao M, Wang F, Li Y, Li H, Zheng J, et al. Integrating choline and specific intestinal microbiota to classify type 2 diabetes in adults: A machine learning based metagenomics study. Front Endocrinol. 2022;13:906310.
118. Sprinkles JK, Lulla A, Hullings AG, Trujillo-Gonzalez I, Klatt KC, Jacobs DR, Jr., et al. Choline metabolites and 15-year risk of incident diabetes in a prospective cohort of adults: Coronary Artery Risk Development in Young Adults (CARDIA) Study. Diabetes Care. 2024;47(11):1985–94.
119. Jia J, Dou P, Gao M, Kong X, Li C, Liu Z, et al. Assessment of causal direction between gut microbiota–dependent metabolites and cardiometabolic health: A bidirectional Mendelian randomization analysis. Diabetes. 2019;68(9):1747–55.
120. Miao J, Ling A, Manthena P, Gearing M, Graham M, Crooke R, et al. Flavin-containing monooxygenase 3 as a potential player in diabetes-associated atherosclerosis. Nature Commun. 2015;6:6498.
121. Wu K, Yuan Y, Yu H, Dai X, Wang S, Sun Z, et al. The gut microbial metabolite trimethylamine N-oxide aggravates GVHD by inducing M1 macrophage polarization in mice. Blood. 2020;136(4):501–15.
122. Seldin MM, Meng Y, Qi H, Zhu W, Wang Z, Hazen SL, et al. Trimethylamine N-oxide promotes vascular inflammation through signaling of mitogen-activated protein kinase and nuclear factor-κB. J Am Heart Assoc. 2016;5(2):e002767.
123. Carabalí-Isajar ML, Rodríguez-Bejarano OH, Amado T, Patarroyo MA, Izquierdo MA, Lutz JR, et al. Clinical manifestations and immune response to tuberculosis. World J Microbiol Biotechnol. 2023;39(8):206.
124. Wang Z, Klipfell E, Bennett BJ, Koeth R, Levison BS, Dugar B, et al. Gut flora metabolism of phosphatidylcholine promotes cardiovascular disease. Nature. 2011;472:57.
125. Peyron P, Vaubourgeix J, Poquet Y, Levillain F, Botanch C, Bardou F, et al. Foamy macrophages from tuberculous patients' granulomas constitute a nutrient-rich reservoir for *M. tuberculosis* persistence. PLoS Pathog. 2008;4(11):e1000204.
126. Vrieling F, Alisjahbana B, Sahiratmadja E, van Crevel R, Harms AC, Hankemeier T, et al. Plasma metabolomics in tuberculosis patients with and without concurrent type 2 diabetes at diagnosis and during antibiotic treatment. Sci Rep. 2019;9(1):18669.
127. Sanchez-Lopez E, Zhong Z, Stubelius A, Sweeney SR, Booshehri LM, Antonucci L, et al. Choline uptake and metabolism modulate macrophage IL-1β and IL-18 production. Cell Metab. 2019;29(6):1350–62.
128. Al-Sulaiti H, Anwardeen N, Bashraheel SS, Naja K, Elrayess MA. Alterations in choline metabolism in non-obese individuals with insulin resistance and type 2 diabetes mellitus. Metabolites. 2024;14(8):457.
129. Jaworska K, Kuś M, Ufnal M. TMAO and diabetes: From the gut feeling to the heart of the problem. Nutr Diabetes. 2025;15(1):21.
130. Tsikas D. Urinary dimethylamine (DMA) and its precursor asymmetric dimethylarginine (ADMA) in clinical medicine, in the context of nitric oxide (NO) and beyond. J Clin Med. 2020;9(6):1843.
131. Vallance HD, Koochin A, Branov J, Rosen-Heath A, Bosdet T, Wang Z, et al. Marked elevation in plasma trimethylamine-N-oxide (TMAO) in patients with mitochondrial disorders treated with oral l-carnitine. Mol Genet Metab Rep. 2018;15:130–3.
132. Upadhyay A, Boyle KE, Broderick TL. The effects of streptozotocin-induced diabetes and insulin treatment on carnitine biosynthesis and renal excretion. Molecules. 2021;26(22):6872.
133. Hatamkhani S, Khalili H, Karimzadeh I, Abdollahi A, Jafari S, Khazaeipour Z. Carnitine deficiency and its possible risk factors in TB patients: First report. Immunotherapy. 2013;5(9):945–53.
134. Jirillo E, Altamura M, Marcuccio C, Tortorella C, Simone C, Antonaci S. Immunological responses in patients with tuberculosis and in vivo effects of acetyl-L-carnitine oral administration. Mediators Inflamm. 1993;2:S17–20.

135. Jirillo E, Altamura M, Munno I, Pellegrino NM, Sabato R, Di Fabio S, et al. Effects of acetyl-L-carnitine oral administration on lymphocyte antibacterial activity and TNF-alpha levels in patients with active pulmonary tuberculosis. A randomized double blind versus placebo study. Immunopharmacol Immunotoxicol. 1991;13(1-2):135–46.
136. Park EA, Mynatt RL, Cook GA, Kashfi K. Insulin regulates enzyme activity, malonyl-CoA sensitivity and mRNA abundance of hepatic carnitine palmitoyltransferase-I. Biochem J. 1995;310(Pt 3):853–8.
137. Stam SP, Eisenga MF, Gomes-Neto AW, van Londen M, de Meijer VE, van Beek AP, et al. Muscle mass determined from urinary creatinine excretion rate, and muscle performance in renal transplant recipients. J Cachexia Sarcopenia Muscle. 2019;10(3):621–9.
138. Tynkevich E, Flamant M, Haymann J-P, Metzger M, Thervet E, Boffa J-J, et al. Decrease in urinary creatinine excretion in early stage chronic kidney disease. PLoS One. 2014;9(11):e111949.
139. Ávila M, Mora Sánchez MG, Bernal Amador AS, Paniagua R. The metabolism of creatinine and its usefulness to evaluate kidney function and body composition in clinical practice. Biomolecules. 2025;15(1):41.
140. Yokozawa T, Fujitsuka N, Oura H. Variations in the distribution of methylguanidine with the progression of renal failure after methylguanidine loading. Nephron. 2008;52(4):347–51.
141. Nagashima K, Yagi H, Yutani S, Miyake H, Onigata K, Kuroume T. Relationship Between Serum Levels of Methylguanidine and Glycemic Control in IDDM Children. Diabetes Care. 1993;16(8):1196-8.

Figures

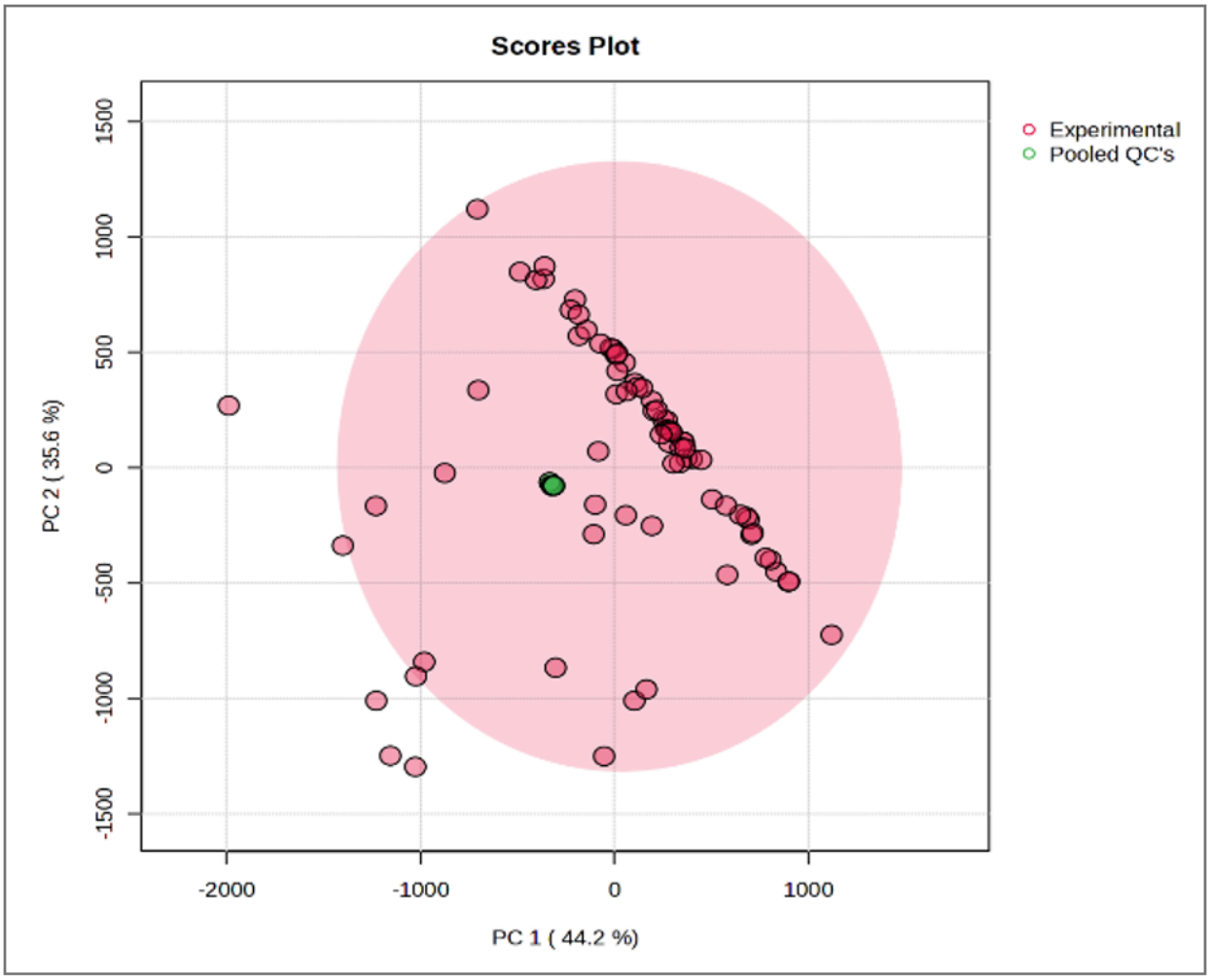


Figure 1

PCA plot of QC's and experimental samples shows tight clustering of QC samples. The tight clustering of the pooled QC samples indicates the absence of a batch effect.

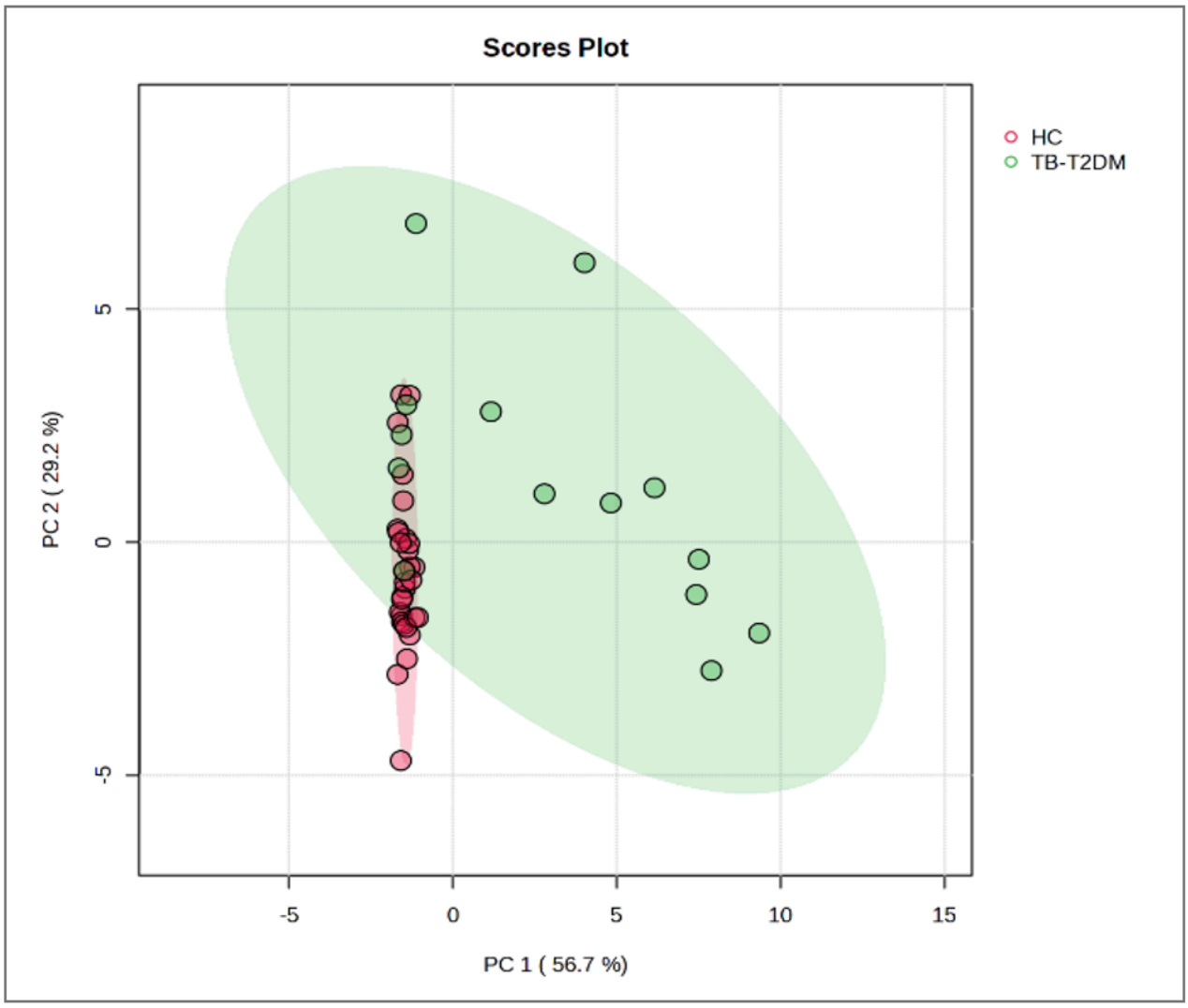


Figure 2

PCA plot showing partial separation between the HC and TB-T2DM cohorts. The significant separation between TB-T2DM samples indicates substantial intragroup heterogeneity, while the tight clustering of the HC's indicates significant homogeneity in this group.

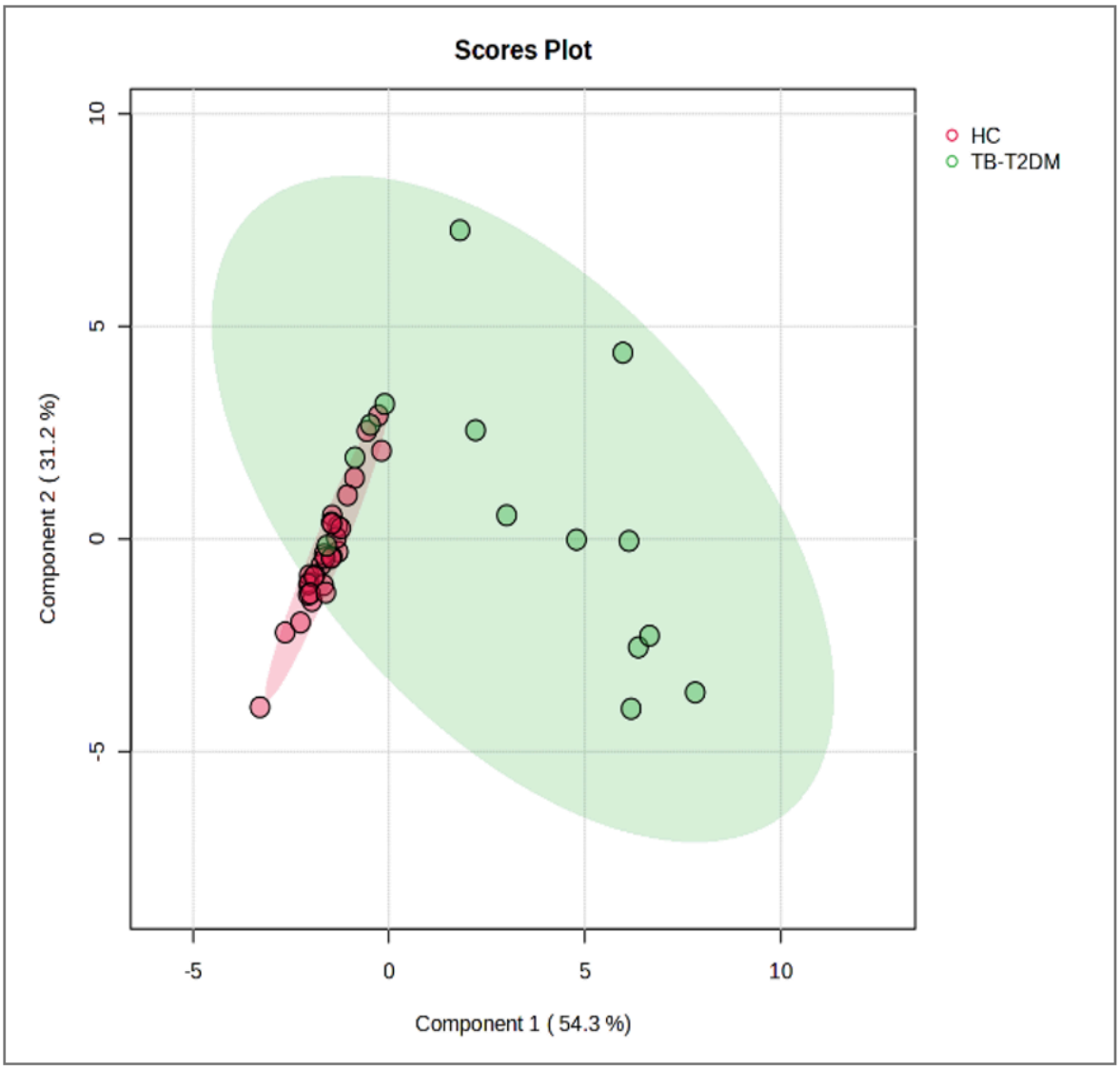


Figure 3

PLS-DA plot of TB-T2DM patients versus HCs showing partial separation between these cohorts. The tight clustering of HC's shows intragroup homogeneity, while separation between TB-T2DM samples shows significant heterogeneity in this group.

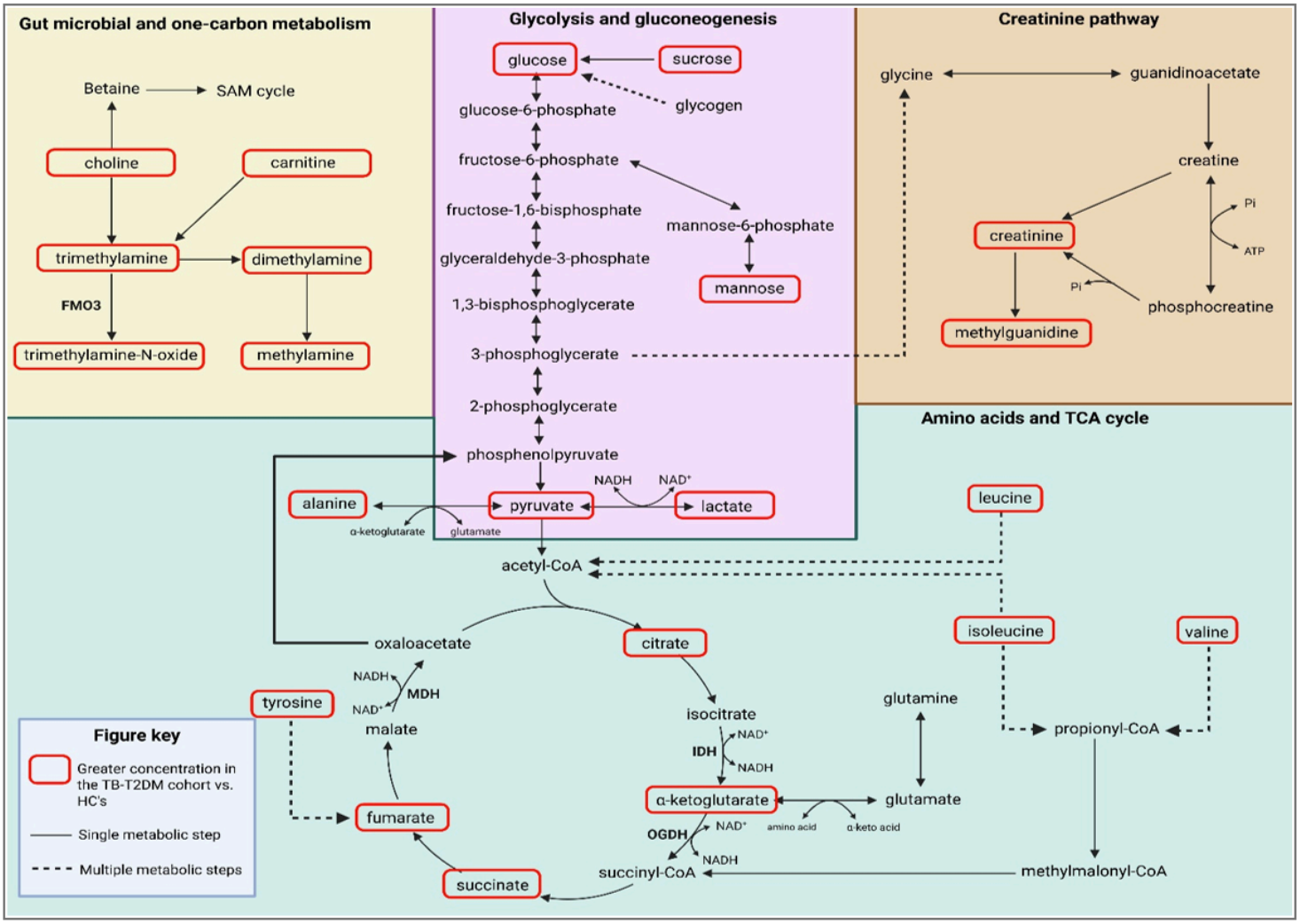


Figure 4

A metabolic map illustrating the metabolites with significant alterations in TB-T2DM patients relative to HCs. NAD^+ = oxidised nicotinamide adenine dinucleotide; NADH = reduced nicotinamide adenine dinucleotide; IDH = isocitrate dehydrogenase; OGDH = oxoglutarate dehydrogenase; MDH = malate dehydrogenase; FMO3 = flavin-containing monooxygenase 3; CoA = coenzyme-A; P_i = phosphate moiety; ATP = adenosine triphosphate; TCA = tricarboxylic acid.